

# Structural and Magnetic Properties of Magnetic Spinel Ferrite ( $\text{Cu}_x\text{Mg}_{1-x}\text{Fe}_2\text{O}_4$ ) $0.0 \leq x \leq 0.9$ Nano-Particles

**Sameer H. AL-Nesrawy**, University of Babylon, College of Education for Pure Sciences, Department of Physics (Babylon, Iraq)

**Najlaa M. Awad**, University of Babylon, College of Education for Pure Sciences, Department of Physics (Babylon, Iraq)

**Ammar Y. AL-Mamoori**, University of Babylon, College of Education for Pure Sciences, Department of Physics (Babylon, Iraq)

**Jassim M. AL-Issawe**, University of Babylon, College of Education for Pure Sciences, Department of Physics (Babylon, Iraq)

**Mohammed H. AL-Maamori**, University of Babylon, College of Engineering Materials, Department of Polymers engineering, (Babylon, Iraq)

## Article Info

Volume 83

Page Number: 12864 - 12873

Publication Issue:

March - April 2020

## Abstract:

In this work, magnesium copper spinel ferrite ( $\text{Cu}_x\text{Mg}_{1-x}\text{Fe}_2\text{O}_4$ ;  $x = 0.0, 0.1, 0.3, 0.5, 0.7, 0.9$ ) nano-composites were prepared successfully by the sol-gel method.  $\text{Mg}(\text{NO}_3)_2 \cdot 6\text{H}_2\text{O}$ ,  $\text{Fe}(\text{NO}_3)_3 \cdot 9\text{H}_2\text{O}$  and  $\text{Cu}(\text{NO}_3)_2 \cdot 3(\text{H}_2\text{O})$  were used as the source of divalent ( $\text{Mg}^{2+}$  and  $\text{Co}^{2+}$ ) and trivalent ( $\text{Fe}^{3+}$ ) cations, respectively and urea were used as the reducing agent. The effect of  $\text{Cu}^{+2}$  ion on magnetic and structural properties of ferrite  $\text{Cu}_x\text{Mg}_{1-x}\text{Fe}_2\text{O}_4$  nano-composite were investigated. The test methods obtained by XRD, SEM, TEM, EDX, FT-IR spectroscopy and VSM. The results showed that the final products consist spinel phase (Fd3m (227)) cubic with particles similar sphere nano-particles. Also observed that the increase doping of  $\text{Cu}^{+2}$  concentration it has big effect on the (Ms) of the  $\text{Cu}_x\text{Mg}_{1-x}\text{Fe}_2\text{O}_4$  spinel ferrite nano-particles. The Magnetic properties of  $\text{Cu}_x\text{Mg}_{1-x}\text{Fe}_2\text{O}_4$  spinel ferrite where ( $x=0.0, 0.1, 0.3, 0.5, 0.7, 0.9$ ) was studied at room-temperature this was done by measuring (M-H hysteresis loop curves). Also all samples have been soft magnetic properties that is dependent of (Cu-Mg) content.

## Article History

Article Received: 24 July 2019

Revised: 12 September 2019

Accepted: 15 February 2020

Publication: 19 April 2020

**Keywords:** Spinel ferrite, Nanoparticles, sol-gel technolog, , XRD, SEM, TEM, EDX, FT-IR spectroscopy and VSM.

## Introduction:

In recent years, all applications of nonmagnetic materials have been achieved for is due to reason have unique properties [1-5]. So spinel ferrites have been introduced in many applications Recently, spherical fractions have been introduced in many applications, including their use in attenuating microwave within different ranges [6,7]. One of the characteristics of magnetic materials is their permanent magnetism, which can be classified into three types depending on the structural properties is the (soft ferrite, garnet ferrite and hard ferrite) [8,9]. Magnetic materials are used mainly in many

applications, including (magnetic tubes and core transformers, insulating, and generators) [10-11]. Cu-Mg Ferrites Nonmagnetic materials are also used as good filters in resonance imaging as well as in medicine and in many other uses, because of the high magnetic susceptibility used in a wide range of frequencies cost effective, electrical resistance, and good environments stability [12-14].

The only effective way scientists have used to change magnetic properties is to substituted transition metal (Cr, Zn, Mn and Mg, etc.) to spinel ferrite. Also doping the magnetic  $\text{Cu}^{+2}$ ,  $\text{Mn}^{+2}$ , etc. In spinel ferrite this is change chemical properties,

this means mainly the distribution of both divalent and trivalent cations between (tetrahedral –A , octahedral –B) sites[15-17].

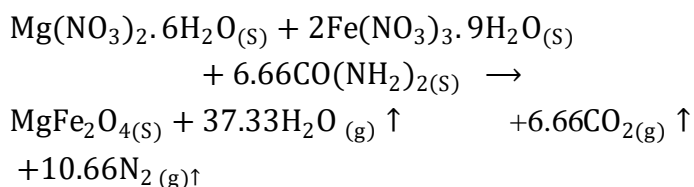
One of the effective ways to control of the internal microstructure of the ferrite obtained nano-particles form, particle size and porosity, etc.

## 2. Experimental

### 2.1. Materials and methods

All chemicals used in this study were obtained from the Indian company Maersk and were used without any further modification. Magnesium nitrate, copper nitrate, iron nitrate and urea were used in this study as fuel for agent. The samples were prepared by adding different molar concentrations of copper ion ( $Cu_xMg_{1-x}Fe_2O_4$ ;  $x = 0.0, 0.1, 0.3, 0.5, 0.7, 0.9$ ) to  $MgFe_2O_4$ . In this case of  $MgFe_2O_4$ , the reaction mixture was taken from the corresponding solutions in a silica mold. The mixture was treated at  $600^\circ C$  for 2 hours at  $5^\circ C/min$ . After the solution becomes solid and the self-combustion process is completed, the resulting solution is washed with water and dried at a temperature  $50^\circ C$  for an hour.

The samples prepared of ( $Cu_xMg_{1-x}Fe_2O_4$ ;  $x = 0.0, 0.1, 0.3, 0.5, 0.7, 0.9$ ) ferrite were taken following shape  $MgFe_2O_4, Cu_{0.1}Mg_{0.9}Fe_2O_4, Cu_{0.3}Mg_{0.7}Fe_2O_4, Cu_{0.5}Mg_{0.5}Fe_2O_4, Cu_{0.7}Mg_{0.3}Fe_2O_4, Cu_{0.9}Mg_{0.1}Fe_2O_4$ , respectively and the interaction can be written as follows;



### 2.2 Techniques

structural properties of ( $Cu_xMg_{1-x}Fe_2O_4$ ;  $x = 0.0, 0.1, 0.3, 0.5, 0.7, 0.9$ ) ferrite nano particle samples were performed using a shimadzu XRD-6000 with

$Cu - K\alpha_1$  radiation and  $\lambda = 1.5405 \text{ \AA}$  at  $40kV$  and  $30mA$ . Structural refinements using the rietveld method were using PDXL program, also and both refined lattice parameters and crystalline size of the obtained ferrites were reported. The surface functional groups were analyzed by thermal (FT-IR) spectrometer. The samples were incorporated in KBr pellets for the measurements. Morphological studies and (EDX) analysis have been performed with a Joel JSM-6360 high-resolution (SEM). Measurements of (TEM) have been performed by Philips TEM (CM20). UV-Visible spectrum of the diffuse reflectance using Cary -NIR UV-visible spectro-photometer to estimate band gap energy (Eg). Magnetic properties measurement at room temperature using a vibrating sample magneto-meter (VSM) model (PMC Micro-Mag 3900 equipped with 1 T magnet).

## 3. Results and discussion

### 3.1 Scanning electron microscope (SEM) and (EDX) measurements

Figure.1 showed the Scanning electron microscope (SEM) image and (EDX) analyses of ( $Cu_xMg_{1-x}Fe_2O_4$ ;  $x = 0.0, 0.1, 0.3, 0.5, 0.7, 0.9$ ) spinel ferrite nano-particle. (Figure. 1 a, b and c) shows a picture of the pure sample  $MgFe_2O_4, Cu_{0.7}Mg_{0.3}Fe_2O_4$  and  $Cu_{0.9}Mg_{0.1}Fe_2O_4$  nano-particle, respectively. Also observed the array of magnetic nano-particles has been formed with microstructure features like to spherical geometry. Because of magnetic dipole interactions between the ferrite particles, the bloc also saw to some extent. Average size of diameter particles of the spectra of pure  $MgFe_2O_4, Cu_{0.7}Mg_{0.3}Fe_2O_4$  and  $Cu_{0.9}Mg_{0.1}Fe_2O_4$  nano-particle in the range 19nm-25nm as shown in (Fig.1(d,e and f)). EDX spectra confirmed the purity of the product as well as the presence of iron, copper, oxygen and magnesium.

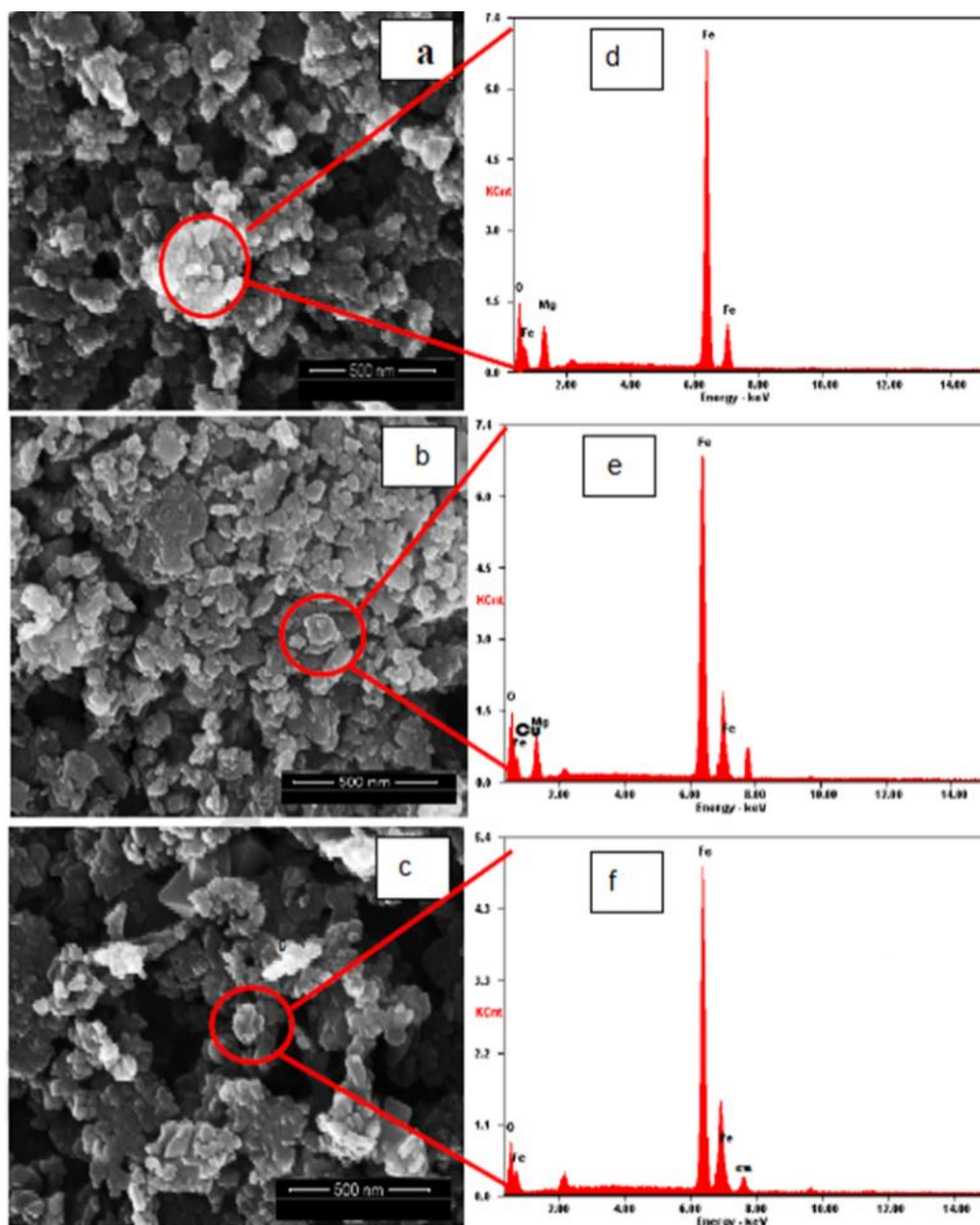


**Figure.1** SEM image of  $\text{Cu}_x\text{Mg}_{1-x}\text{Fe}_2\text{O}_4$ : $x=0.0,0.7,0.9$  spinel ferrite are a,b,c respectively and EDX analysis of  $\text{Cu}_x\text{Mg}_{1-x}\text{Fe}_2\text{O}_4$ : $x=0.0,0.7,0.9$  are d, e, f respectively.

### 3.2 X-ray Powder Analysis

The structural properties of ferrite powder were investigating by the XRD patterns. Figure.2, explained the XRD patterns of  $\text{MgFe}_2\text{O}_4$ ,  $\text{Cu}_{0.7}\text{Mg}_{0.3}\text{Fe}_2\text{O}_4$  and  $\text{Cu}_{0.9}\text{Mg}_{0.1}\text{Fe}_2\text{O}_4$  ferrite nano-particle and also showed that the spinel ferrite phase forms and is cubic. Structure.Rietveld

refinement was used to determine all spectra and lattice parameters. And also we note that the  $hkl$  values match exactly with (JCPDS Card Number.71-1233 for  $\text{MgFe}_2\text{O}_4$  samples without any impurities and all samples exhibit single phase with Fd3m group [18,19]. les exhibit single phase with Fd3m group [34,35].

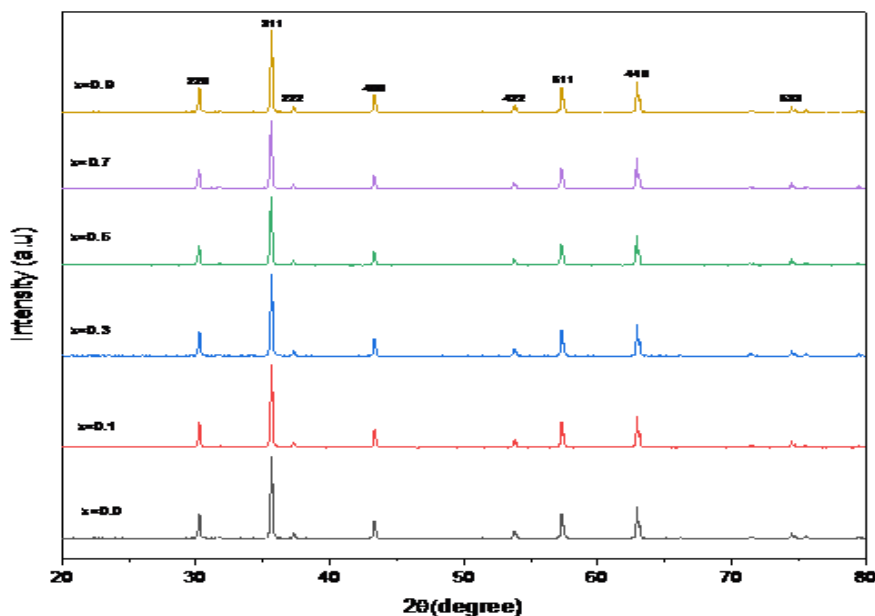


**Figure .2** XRD patterns of  $Cu_xMg_{1-x}Fe_2O_4$ :  $x$  0.0,0.1,0.3,0.5,0.7,0.9) spinel ferrite samples

The particle size of led to decrease the particle size from 20.3 -16.59nm ( $Cu_xMg_{1-x}Fe_2O_4$ :  $x$  0.0,0.1,0.3,0.5,0.7,0.9) spinel Because increasing the concentration of ferrite nano-particle calculated by Debye Scherer's nanoparticles within the material increases its equation and found for un doped  $MgFe_2O_4$  particle size and thus has good properties. .However, the increase  $Cu^{+2}$  concentration that is

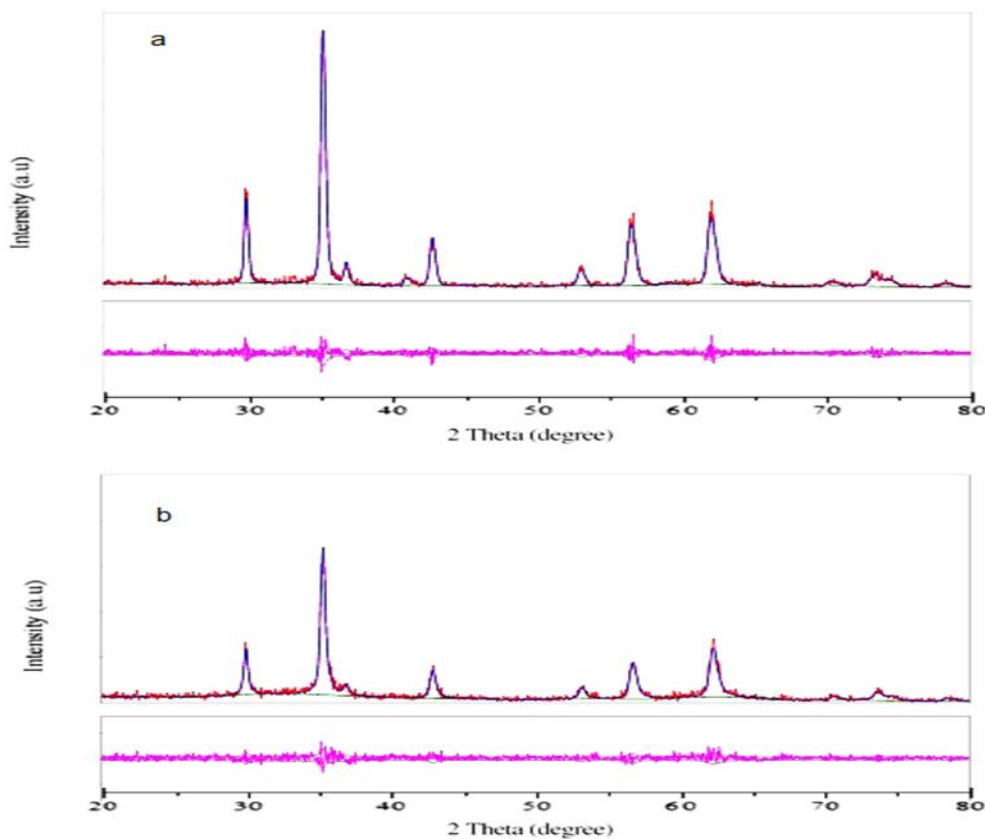


**Figure.3** Rietveld refinement XRD method of  $Cu_xMg_{1-x}Fe_2O_4$ , a( $x=0.0$ ) and b( $x=0.9$ )

The Rietveld analyses and (XRD) analyses as shown in figure in (Fig.3). The Particle size and refined structural coefficients for all samples were shown in Table.1, Figure.4. The lattice coefficient value was obtained for undoped of  $\text{MgFe}_2\text{O}_4 = 8.303 \text{ \AA}$  this value is not fixed but is increasing from 8.309 -8.331 With increased of copper ion content (0.1 to 0.7)

thus corresponds with the Vegard's law [36]. The smaller increasing in lattice coefficient is due to replacement of the smaller manganese ion radius ( $0.64 \text{ \AA}$ ) by the larger ionic radius ( $\text{Cu}^{+2}$ ,  $0.70 \text{ \AA}$ ) in the system ( $\text{Cu}_x\text{Mg}_{1-x}\text{Fe}_2\text{O}_4$  spinel ferrite) [20,21].

**Table.1:** Lattice parameter and crystallite size (Scherer formula, Rietveld analysis) of spinel ferrite  $\text{Cu}_x\text{Mg}_{1-x}\text{Fe}_2\text{O}_4$  ( $x = 0.0, 0.1, 0.3, 0.5, 0.7, 0.9$ )

Samples	Lattice parameters ( $\text{\AA}$ )	Crystallite size (nm)	
	Rietveld analysis	Scherer Formula	Rietveld analysis
$\text{MgFe}_2\text{O}_4$	8.403	21.23	21
$\text{Cu}_{0.1}\text{Mg}_{0.9}\text{Fe}_2\text{O}_4$	8.409	20.43	20
$\text{Cu}_{0.3}\text{Mg}_{0.7}\text{Fe}_2\text{O}_4$	8.413	19.68	19
$\text{Cu}_{0.5}\text{Mg}_{0.5}\text{Fe}_2\text{O}_4$	8.421	15.59	17
$\text{Cu}_{0.7}\text{Mg}_{0.3}\text{Fe}_2\text{O}_4$	8.429	16.54	19
$\text{Cu}_{0.9}\text{Mg}_{0.1}\text{Fe}_2\text{O}_4$	8.431	18.69	19

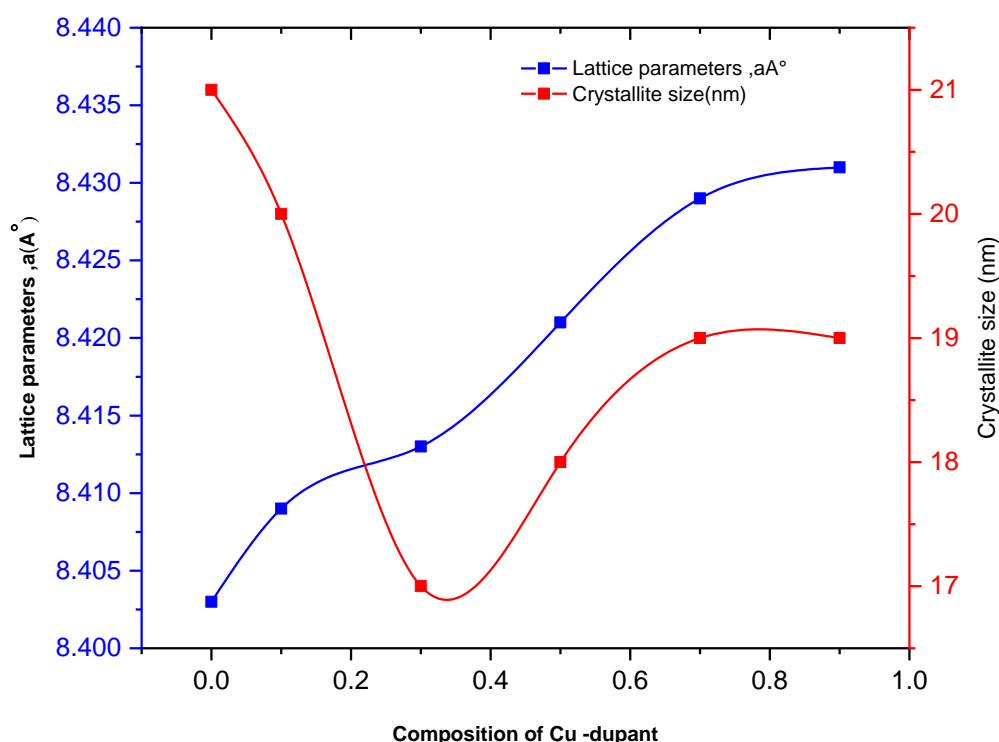


**Figure.4** lattice parameter and crystallite size of of spinel ferrite  $\text{Cu}_x\text{Mg}_{1-x}\text{Fe}_2\text{O}_4$  ( $x = 0.0, 0.1, 0.3, 0.5, 0.7, 0.9$ ) nano-particles

### 3.3 (TEM) and (SAED) Analysis

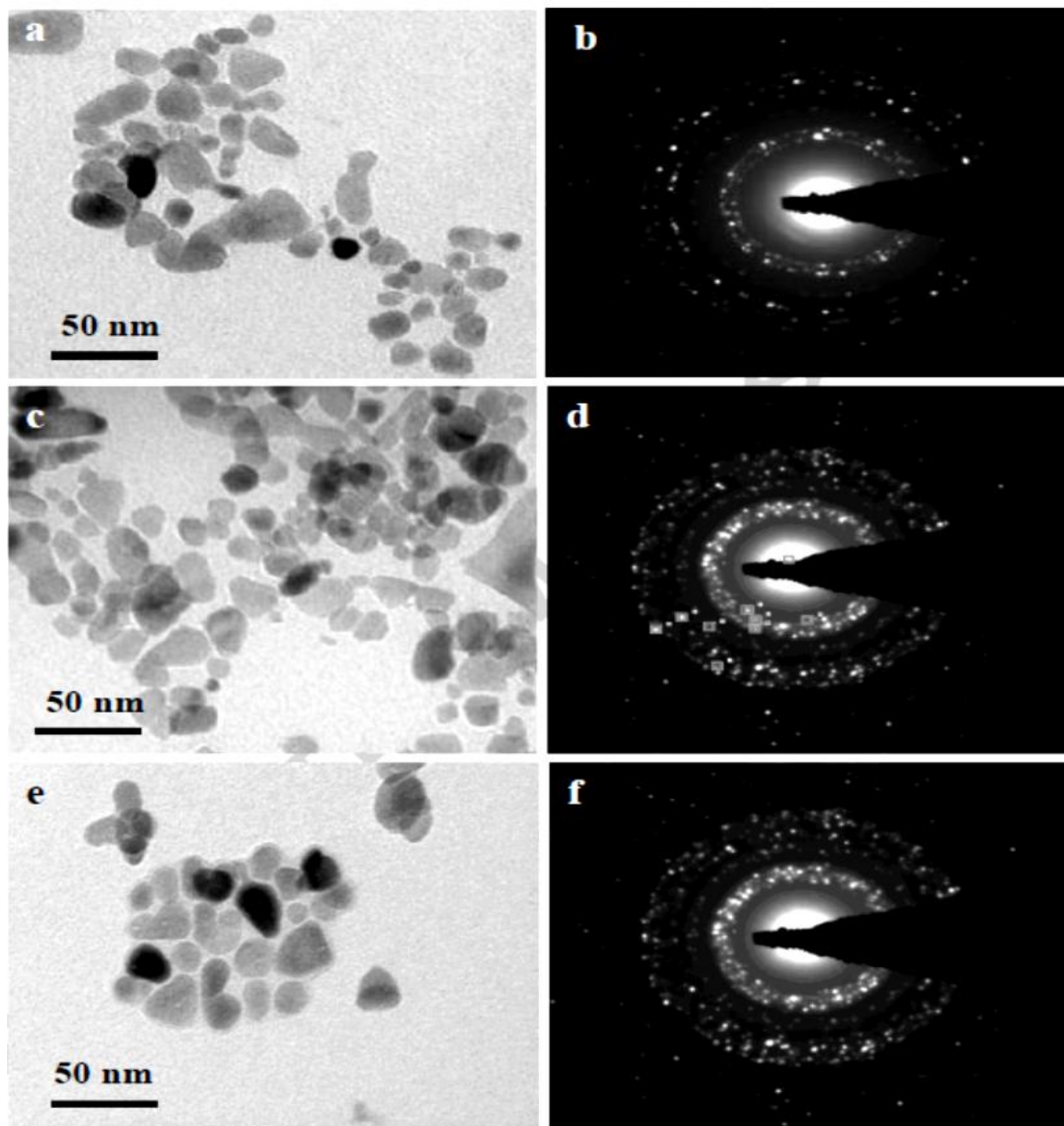


**Figure.5** show the TEM images of  $Cu_xMg_{1-x}Fe_2O_4$ , a,c, and e ( $x=0.0,0.7,0.9$ ) samples, respectively and (SAED) of  $Cu_xMg_{1-x}Fe_2O_4$ , b,d and f ( $x=0.0,0.7,0.9$ ) samples, respectively

Transmission electron Microscope (TEM) They were used to showed morphology of  $Cu_xMg_{1-x}Fe_2O_4$  spinel ferrite nano-particles (Fig.5 a,c and e ) showed that the (TEM) picture of the pure sample  $MgFe_2O_4, Cu_{0.7}Mg_{0.3}Fe_2O_4$  and  $Cu_{0.9}Mg_{0.1}Fe_2O_4$  spinel ferrite nano-particle ,

respectively with the particle size 24nm .(Fig.5 b,d and f ) showed the (SAED) patterns of the pure sample  $MgFe_2O_4, Cu_{0.7}Mg_{0.3}Fe_2O_4$  and  $Cu_{0.9}Mg_{0.1}Fe_2O_4$  spinel ferrite nano-particle ,respectively, confirm the crystalline nature of nanoparticles with a high purity.

### 3.4 (FT-IR) spectroscopy analysis

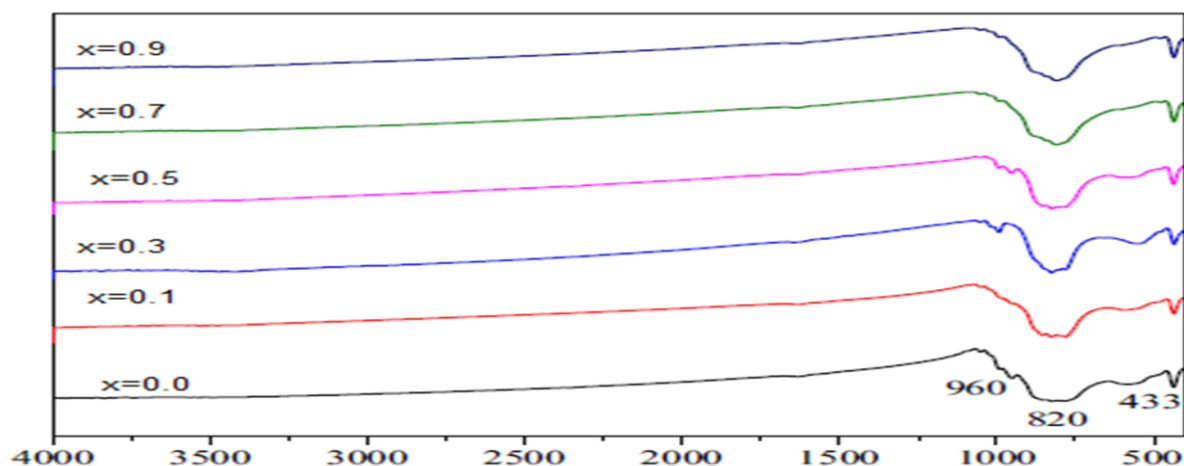


**Figure.6** FT-IR spectra of spinel ferrite  $Cu_xMg_{1-x}Fe_2O_4$  ( $x=0.0,0.1,0.3,0.5,0.7,0.9$ ) nanoparticles

We used the measurement (FT-IR) to check for functional groups of the samples (FT-R) spectra bands observed. (Fig.6) showed that the spectrum of (FT-IR) of  $Cu_xMg_{1-x}Fe_2O_4$  spinel ferrite where ( $x=0.0,0.1,0.3,0.5,0.7,0.9$ ). FT-IR spectra indicated that the spinel ferrite magnetic nano-particles spinel cubic structure, this is due to the peaks can be observed at the frequency range from ( $430cm^{-1}$  -  $830cm^{-1}$ ) bonds at (tetrahedral(A), octahedral (B) sites), respectively. Well we can say that the (FT-IR) results were good compatible with (Rietveld analysis and XRD analysis).

### 3.6 Magnetic Properties

The Magnetic properties of  $Cu_xMg_{1-x}Fe_2O_4$  spinel ferrite where ( $x=0.0,0.1,0.3,0.5,0.7,0.9$ ) was

studied at room-temperature this was done by measuring (M-H hysteresis loop curves) shown in (Fig.7). Also all samples has soft magnetic properties that is dependent of (Cu-Mg) content. And also observed from (M-H hysteresis loop curves) that the content of  $Cu^{+2}$  ions increase, also both ( $M_s$  and  $M_r$ ) (saturation magnetization and coactivity values) increased. As shown in (Table.2, Figure.8), This is due to the  $Cu^{+2}$  ions was have better magnetic properties  $3\mu_B$  that is substitute zero magnetic properties of  $Mg^{+2}$  ions -  $0\mu_B$  [22,23]. Where it is known that the magnetization is determined by (A and B) sites, there is equal ( $M=M_B - M_A$ ).

**Table 2.** Variation of coercivity ( $H_c$ ), remanant magnetization ( $M_r$ ) and saturation magnetization ( $M_s$ ) of spinel ferrite  $Cu_xMg_{1-x}Fe_2O_4$   $x = 0.0,0.1,0.3,0.5,0.7,0.9$

Samples	$H_c$ (Oe)	$M_r$ (emu/g)	$M_s$ (emu/g)
$MgFe_2O_4$	95.70	1.53	3.784
$Cu_{0.1}Mg_{0.9}Fe_2O_4$	96.20	3.14	8.654
$Cu_{0.3}Mg_{0.7}Fe_2O_4$	96.66	6.73	23.76
$Cu_{0.5}Mg_{0.5}Fe_2O_4$	98.40	7.68	36.65
$Cu_{0.7}Mg_{0.3}Fe_2O_4$	98.30	8.87	50.14
$Cu_{0.9}Mg_{0.1}Fe_2O_4$	99.14	9.65	63.43

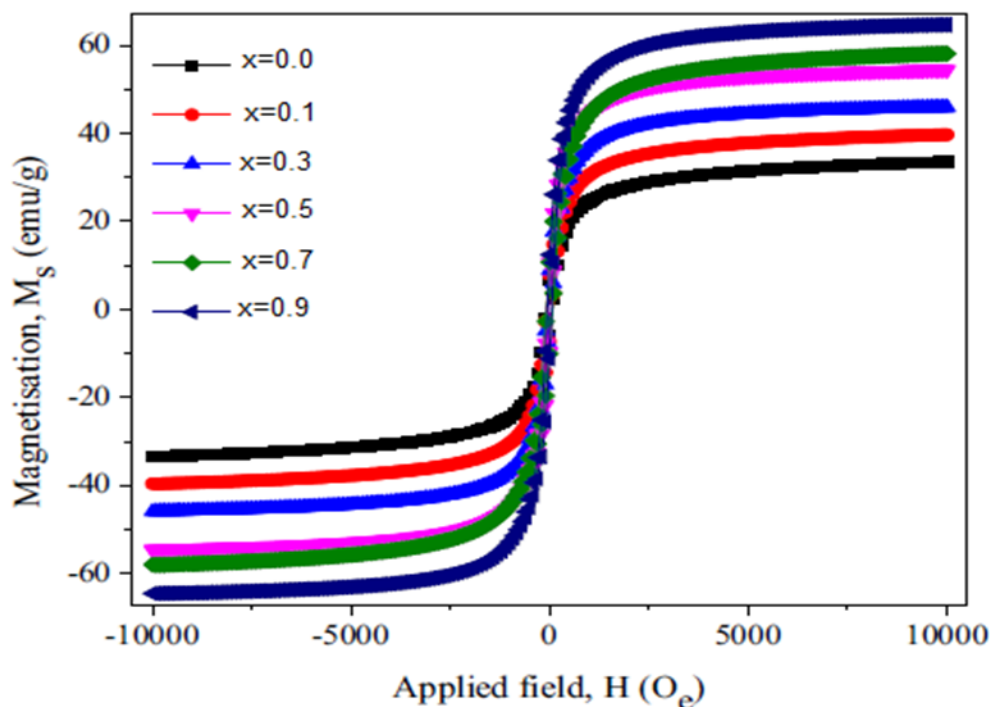


**Figure.7** The hysteresis loop of spinel ferrite  $Cu_xMg_{1-x}Fe_2O_4$  ( $x=0.0,0.1,0.3,0.5,0.7,0.9$ ) nanoparticles

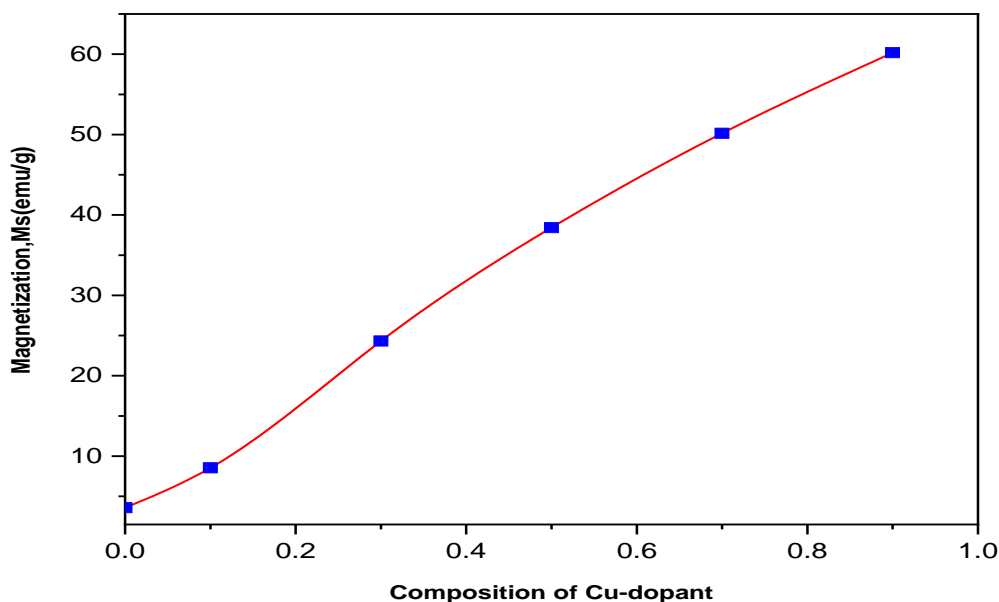


**Figure.8** The Saturation magnetization ( $M_s$ ) of of spinel ferrite  $Cu_xMg_{1-x}Fe_2O_4$  ( $x=0.0,0.1,0.3,0.5,0.7,0.9$ ) nanoparticle

**Conclusions and Recommendations**

$Cu_xMg_{1-x}Fe_2O_4$  spinel ferrite where ( $x=0.0,0.1,0.3,0.5,0.7,0.9$ ) nano-particles were successfully synthesized by the sol-gel technology.

The effect of  $Cu^{+2}$  ion on (Magnetic and structural properties of ferrite  $Cu_xMg_{1-x}Fe_2O_4$  nano-composite were investigated. Structural, morphological properties, magnetic, element



composition, and functional group were studied by the (XRD, SEM, TEM, VSM, EDX, and FT-IR). The magnetic characterization of  $\text{Cu}_x\text{Mg}_{1-x}\text{Fe}_2\text{O}_4$  ( $x=0.0, 0.1, 0.3, 0.5, 0.7, 0.9$ ) nano-particles were studied and found that the spinel ferrite  $\text{Cu}_x\text{Mg}_{1-x}\text{Fe}_2\text{O}_4$  ( $0.0 \leq x \leq 0.9$ ) nano-particles have been smaller hysteresis loop. And also we note that the *hkl* values match exactly with (JCPDS Card Number. 71-1233 for  $\text{MgFe}_2\text{O}_4$  samples without any impurities and all samples exhibit single phase with Fd-3m space group. The Magnetic properties of  $\text{Cu}_x\text{Mg}_{1-x}\text{Fe}_2\text{O}_4$  spinel ferrite where ( $x=0.0, 0.1, 0.3, 0.5, 0.7, 0.9$ ) was studied at room-temperature this was done by measuring (M-H hysteresis loop curves). Also all samples have been soft magnetic properties that is dependent of (Cu-Mg) content.

## References

1. Kennedy, J., et al., Intrinsic magnetic order and inhomogeneous transport in Gd-implanted zinc oxide. *Physical review B*, 2013. 88(21): p. 214423.
2. Murmu, P., et al., Observation of magnetism, low resistivity, and magnetoresistance in the near-surface region of Gd implanted ZnO. *Applied Physics Letters*, 2012. 101(8): p. 082408.
3. Pardavi-Horvath, M., Microwave applications of soft ferrites. *Journal of Magnetism and Magnetic Materials*, 2000. 215: p. 171-183.
4. Caloz, C. and T. Itoh, *Electromagnetic metamaterials: transmission line theory and microwave applications*. 2005: John Wiley & Sons.
5. Furlani, E.P., *Permanent magnet and electromechanical devices: materials, analysis, and applications*. 2001: Academic press.
6. Deng, H., et al., Monodisperse magnetic single-crystal ferrite microspheres. *Angewandte Chemie*, 2005. 117(18): p. 2842-2845.
7. Nakamura, T., Low-temperature sintering of NiZnCu ferrite and its permeability spectra. *Journal of Magnetism and Magnetic Materials*, 1997. 168(3): p. 285-291.
8. Naito, Y. and K. Suetake, Application of ferrite to electromagnetic wave absorber and its characteristics. *IEEE Transactions on Microwave Theory and Techniques*, 1971. 19(1): p. 65-72.
9. Maaz, K., et al., Synthesis and magnetic properties of cobalt ferrite ( $\text{CoFe}_2\text{O}_4$ ) nanoparticles prepared by wet chemical route. *Journal of Magnetism and Magnetic Materials*, 2007. 308(2): p. 289-295.
10. Pillai, V. and D. Shah, Synthesis of high-coercivity cobalt ferrite particles using water-in-oil microemulsions. *Journal of Magnetism and Magnetic Materials*, 1996. 163(1-2): p. 243-248.
11. Sato, T., et al., Magnetic properties of ultrafine ferrite particles. *Journal of Magnetism and Magnetic Materials*, 1987. 65(2-3): p. 252-256.
12. Mathew, D.S. and R.-S. Juang, An overview of the structure and magnetism of spinel ferrite nanoparticles and their synthesis in microemulsions. *Chemical Engineering Journal*, 2007. 129(1-3): p. 51-65.
13. Mai, A., et al., Ferrite-based perovskites as cathode materials for anode-supported solid oxide fuel cells: Part I. Variation of composition. *Solid State Ionics*, 2005. 176(15-16): p. 1341-1350.
14. Kim, S., et al., Complex permeability and permittivity and microwave absorption of ferrite-rubber composite at X-band frequencies. *IEEE Transactions on Magnetics*, 1991. 27(6): p. 5462-5464.
15. Chen, D.-H. and X.-R. He, Synthesis of nickel ferrite nanoparticles by sol-gel method. *Materials Research Bulletin*, 2001. 36(7-8): p. 1369-1377.
16. Meshram, M., et al., Characterization of M-type barium hexagonal ferrite-based wide band microwave absorber. *Journal of Magnetism and Magnetic Materials*, 2004. 271(2-3): p. 207-214.
17. David, S., S. Hanzelka, and C. Haltom, Ferrite morphology and variations in ferrite content in austenitic stainless steel welds. 1981, Oak Ridge National Lab., TN (USA).
18. Fetisov, Y.K. and G. Srinivasan, Electric field tuning characteristics of a ferrite-piezoelectric microwave resonator. *Applied physics letters*, 2006. 88(14): p. 143503.
19. Shin, J. and J. Oh, The microwave absorbing phenomena of ferrite microwave absorbers. *IEEE Transactions on Magnetics*, 1993. 29(6): p. 3437-3439.

20. Cheng, Z., et al., Structure, ferroelectric properties, and magnetic properties of the La-doped bismuth ferrite. *Journal of Applied Physics*, 2008. 103(7): p. 07E507.
21. Funakawa, Y., et al., Development of high strength hot-rolled sheet steel consisting of ferrite and nanometer-sized carbides. *ISIJ international*, 2004. 44(11): p. 1945-1951.
22. Maensiri, S., et al., A simple route to synthesize nickel ferrite (NiFe<sub>2</sub>O<sub>4</sub>) nanoparticles using egg white. *Scripta materialia*, 2007. 56(9): p. 797-800.
23. Liu, C., et al., Chemical control of superparamagnetic properties of magnesium and cobalt spinel ferrite nanoparticles through atomic level magnetic couplings. *Journal of the American Chemical Society*, 2000. 122(26): p. 6263-6267.
24. Abraham, A.G., et al., Enhanced magneto-optical and photo-catalytic properties of transition metal cobalt (Co<sup>2+</sup> ions) doped spinel MgFe<sub>2</sub>O<sub>4</sub> ferrite nanocomposites. *Journal of Magnetism and Magnetic Materials*, 2018. 452: p. 380-388.
25. Manikandan, A., et al., A novel one-pot combustion synthesis and opto-magnetic properties of magnetically separable spinel Mn<sub>x</sub>Mg<sub>1-x</sub>Fe<sub>2</sub>O<sub>4</sub> (0.0 ≤ x ≤ 0.5) nanophotocatalysts. *Journal of Superconductivity and Novel Magnetism*, 2015. 28(4): p. 1405-1416.